LA-UR-96-2434

Title: REGIONAL CHARACTERIZATION OF WESTERN CHINA-II

CONF-9609185--13

Author(s): G. E. Randall, EES-3
H. E. Hartse, EES-3
W. Scott Phillips, EES-3
S. R. Taylor, EES-3

Submitted to: 18th Research Symposium on Monitoring Comprehensive Test Ban Treaty, 4-6 September 1996, Annapolis, Maryland.

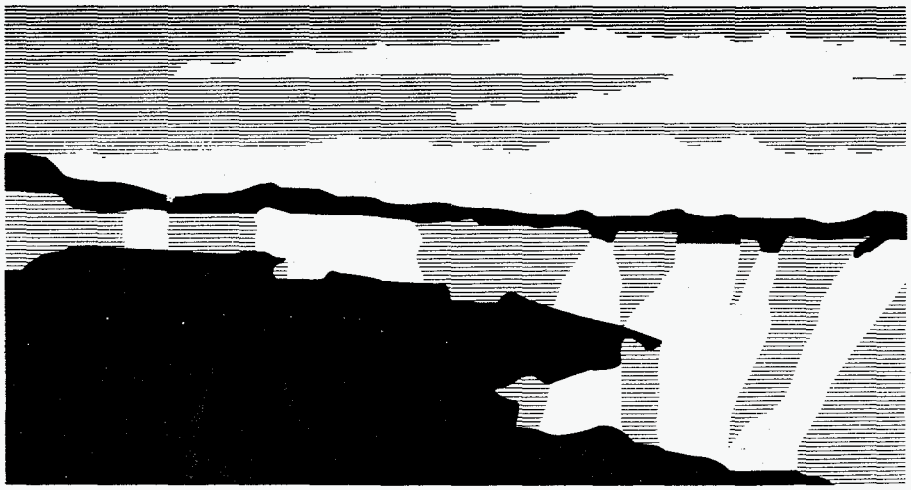

Los Alamos
NATIONAL LABORATORY

Form No. 836 R5
ST 2629 10/91

DISCLAIMER

Regional Characterization of Western China - II

G.E. Randall, H.E. Hartse, W.S. Phillips, and S.R. Taylor,
Geophysics Group EES-3, Los Alamos National Laboratory

Sponsored by the U.S. Department of Energy, Contract W-7405-ENG-36
Comprehensive Test Ban Treaty Research and Development Program, ST482A

ABSTRACT

As part of the CTBT Research and Development regional characterization effort, geological, geophysical, and seismic data are being assembled and organized for inclusion in a knowledge base for China. We have continued our analysis using data from the station WMQ of the Chinese Digital Seismic Network (CDSN) and the IRIS station AAK. We are also acquiring and analyzing data from stations that are designated as (or near a designated) primary or secondary CTBT monitoring station including MAK, KURK, NVS, TLG, NIL, LSA, TLY, ULN, HIA, MDJ, LZH, XAN, ENH, and KMI. Additional stations will be included as time permits. Regional seismograms are being analyzed to construct travel time curves, velocity models, attenuation characteristics, and to quantify regional propagation effects such as phase blockages. Using locations from the USGS Preliminary Determination of Epicenters (PDE) we have identified Pn, Pg, Sn, and Lg phases, constructed travel time curves, and estimated apparent velocities using linear regression. Amplitudes for the seismic phases have been measured using bandpassed waveforms and a series of magnitude relations have been determined for Western China. We have computed detection thresholds for the phases Pn, Pg, Sn, and Lg at WMQ for the frequency bands 1-2 Hz and 4-8 Hz out to 1200 km. Studies of path specific propagation efficiency of the seismic phases have mapped blockages and also identified a possible set of observations that can be used to identify intermediate depth (> 100 km) seismic events in the Pamir-Hindu Kush seismic zone. Chinese seismicity catalogs from the USGS and Chinese State Seismological Bureau (SSB) are being used to identify and obtain seismic data (including mine seismicity) and information for lower magnitude events. Clustering analysis has been used to identify seismicity clusters in space with origin times that are distributed during daylight hours which suggest mining operations. These clusters are being investigated with imagery to attempt to identify precise mine locations.

Key Words: regional seismic characterization, China

OBJECTIVE

We are continuing characterization of the regional excitation and propagation of seismic waves in Western China with sufficient accuracy to explain observed seismic data, and to detect, locate, and discriminate seismic events for the verification of a Comprehensive Test Ban Treaty (CTBT). Our primary source of seismic data for the initial effort has been the stations of the Chinese Digital Seismic Network (CDSN) and IRIS stations. Using seismic waveforms and event locations from the USGS PDE and Chinese seismicity catalogs, we have identified Pn, Pg, Sn, Lg, Love and Rayleigh phases and picked arrival times and amplitudes for the body waves. Analysis of these arrival times will provide travel time and travel time corrections for large well located to improve regional location. Amplitudes are analyzed to calibrate magnitude scales and for use in discrimination research.

RESEARCH ACCOMPLISHED

Seismicity Data (Natural, Explosion and Cultural combined): We have initially used the USGS Preliminary Determination of Epicenters for identifying the seismicity of Western China. For more detailed seismicity with a lower magnitude threshold we have obtained contemporary seismicity catalogs for China. We have recently seen the first results of the translation and tabulation of a more recent set of Chinese seismicity catalogs (1990-1994) for Western China which will allow us to search for waveforms for more recent events too small to be included in the PDE .

Seismic Clusters, Mines?: Figure 1 shows events that are clustered in both space and time. The spatial clustering can be indicative of natural phenomena but the requirement that the events also be clustered in time leads to a presumption of man made events. The small circled cluster on the Russian border is near a known mine. We are identifying possible mine blasts in the Chinese seismicity catalogs using cluster analysis; we searched for spatially clustered epicentral locations in the Chinese seismicity catalog from 1973 through 1989 containing magnitudes as low as 2.0. The clustering required each event to be within 10 km of a minimum of 10 other events. We then examined time-of-day (GMT) histograms of each cluster for unusual behavior. In the circled cluster, all events (over 10 years) occurred in an 8-hour time range, indicating possible, man-made origin. The cluster is within 20 km of Druzhba, a known Russian mining area. We are currently searching for overhead images to confirm and pinpoint the mine location. We will use the same cluster analysis on the more recent Chinese catalogs. Events that are confirmed as mine blasts can be used for discriminant calibration and reference waveforms.

Magnitude Scale Calibration: Figure 2a shows a magnitude scale based on linear regression of measured amplitudes for Lg phase measured at WMQ for distances ranging from about 330 km to 1000 km. Magnitude is an important, decision making parameter and we need an estimate that is tied to a broadly used magnitude scale, such as teleseismic mb. The Chinese magnitudes are unreliable, which can be seen by comparing with mb for larger (>3.8) events. Figure 2a illustrates our method using broad-band vertical Lg phase bandpassed from 1-2 Hz. We find a least-squares fit to PDE mb ($3.8<mb<6.2$) using the formula mb = log(amplitude) + a + b log(distance) for rms amplitude in nanometers/sec and distance km for events with signal-to-(pre-Pn)noise > 10. In Figure 2b we show a comparison of magnitude estimates using phases Pn, Pg, Sn, and Lg in each of 4 frequency passbands, showing the residual variance of the regression estimate. Pg, Lg and Sn

are all nearly equivalent. The percentage of observed seismic data with S/N > 10 in the 4 frequency passbands is also shown. The second figure summarizes fits for Pn, Pg, Sn and Lg, for four, octave-width, frequency bands. The best band is 1-2 Hz, best phases Sn and Lg with Pg not far behind. The mb residuals for different phases and bands are positively correlated, indicating little improvement to mb estimates are possible by combining information.

Propagation Effects: Figure: 3a shows Lg phase propagation efficiency to station AAK. The region south of AAK shows closely spaced events that show some efficient and some poor propagation of Lg to AAK. The distance range seems too short to be a structural effect. The region also includes some intermediate depth (>100km) seismicity so the problem may be a source effect, not a structural blockage of energy. The phase transmission maps are obtained by comparing the rms amplitude of the phase with the rms amplitude of a "pre-phase noise window". The noise window is generally 10-20 seconds long and sits just before the start of the actual phase window. In Figure 3b we show a seismogram comparison of an event with efficient Lg propagation to AAK with a nearby event with poor Lg propagation to AAK. Traces are short period vertical, long period vertical, and long period tangential in each case. On the left the Lg is observed on the short period vertical as well as surface waves on the long period components. On the right the Lg is not observed on the short period vertical and surface waves are not observed on either long period component. The event on the right is probably an intermediate depth event with negligible surface wave excitation, and is difficult to classify with many discriminants. Events in this region have been analyzed (Mellors et al. 1995, Pavlis and Hamburger. 1991) and the existence of intermediate depth events is well established. PDE bulletins generally list depths for many of these small events at 33 km, which is unreliable. We need to find useful ways to characterize the intermediate depth events such as the possible lack of both Rayleigh and Love waves. Propagation effects must be carefully distinguished from source effects. We are also following the results of other groups (Hearn and Ni 1996, McNamara et al. 1995, and McNamara et al. 1996) that are also characterizing regional wave propagation in Western China.

Detection Threshold Analysis: Recent work has shown the effectiveness of various regional discriminants in western China such as P_g/L_g in different frequency bands (Hartse *et al.*, 1996). Given this information, it is important to have a knowledge of detection thresholds for the different regional phases used for discrimination as a function of frequency. We have computed detection thresholds for the phases P_n, P_g, S_n, and L_g at the Chinese Digital Seismic Station (CDSN) station WMQ for the frequency bands 1-2 and 4-8 Hz. As described by Hartse *et al.*, (1996), signal and noise measurements were made for the above-mentioned regional phases from 289 presumed earthquakes recorded at WMQ. Event locations and magnitudes were obtained from both the United States Geological Survey Preliminary Determination of Epicenters (USGS/PDE) catalogs maintained at the Incorporated Research Institutions in Seismology Data Management Center (IRIS DMC) and the Chinese State Seismological Bureau (SSB) for 1988-1989. We are uncertain as to how the magnitudes in the SSB catalogs were calculated. If it is found in subsequent studies that there is a significant offset between worldwide m_b and the magnitudes from the SSB catalog, the calculated detection thresholds will be biased. The distances ranged from less than 100 to about 1200 km and magnitudes ranged from approximately 2.5 to 6.0. In this study, we use peak-to-peak measurements for P_n and RMS measurements for P_g, S_n, and L_g (Hartse, 1995). In computing signal-to-noise ratios (S/N), we use pre-P_n noise measurements (peak-to-peak for P_n S/N and RMS for P_g, S_n, and L_g S/N).

In estimating detection thresholds, we follow the basic technique outlined by Sereno and Bratt (1989). Details are given in (Taylor and Hartse, 1996). Figure 4 shows the 90% detection thresholds for earthquakes recorded at WMQ for the phases P_n, P_g, S_n, and L_g in the 1-2 and 4-8

Hz bands. At a range of 1000 km, the 90% detection threshold for the 4-8 Hz band ranges from 0.4 to 1 magnitude unit greater than the 1-2 Hz band depending on the phase. This, of course, has implications for seismic discriminants such as the P_g/L_g ratio that generally perform better at higher frequencies (e.g. Taylor, 1995; Hartse *et al.,* 1996). The S/N ratios for the P_g/L_g discriminant will be much better in the 1-2 Hz band than the 4-8 Hz band, but the discrimination performance in the 1-2 Hz band is reduced relative to the 4-8 Hz band. At a range of 1000 km we can only expect to be able to construct P_g/L_g discriminants down to a magnitude of approximately 3.5 to 3.8 at 1-2 Hz and 4.5 at 6-8 Hz.

RECOMMENDATIONS AND FUTURE PLANS

We will continue the assembly of regional information, and begin the validation of models by comparing synthetics with real data. Waveform modeling for seismic source and event depth characterization will be attempted. We will continue the collaboration with the discrimination efforts to identify propagation issues and details relevant to discrimination, obtain smaller events identified from regional seismicity catalogs, and mining related events identified from correlation of catalogs with mining. Results we be organized in a form suitable for use by AFTAC in their routine processing and special event studies.

REFERENCES

Hartse, H.E., S.R. Taylor, W.S. Phillips, and G.E. Randall, Regional event discrimination in central Asia with emphasis on western China, *Los Alamos National Laboratory, Los Alamos, NM*, LAUR-96-2002, 45pp, submitted to *Bull. Seism. Soc. Am.*, 1996.

Hearn, T.M., and J.F. Ni, Uppermost mantle structure in Southern Eurasia from Pn tomography and Sn attenuation, AFOSR Final Report, 58 p., 1996.

McNamara, D.E., T.J. Owens, and W.R. Walter, Observation of regional phase propagation across the Tibetan Plateau, *J. Geophys. Res.,* 100, 22,215-22,229, 1995

McNamara, D.E., W.R. Walter, T.J. Owens, and C.J. Ammon, Upper mantle velocity structure beneath the Tibetan Plateau from Pn travel time tomography, *J. Geophys. Res.,* in press,1996

Mellors,RJ, G.L. Pavlis, M.W. Hamburger, and HJ. Al-Shukri, Evidence for a high velocity slab associated with the Hindu Kush seismic zone, *J. Geophys. Res.*, 100, 4067-4078, 1995.

Pavlis, G.L. and M.W. Hamburger, Aftershock sequences of intermediate depth earthquakes in the Pamir-Hindu Kush seismic zone, *J. Geophys. Res.*, 96, 18107-18117, 1991.

Sereno, T.J. and S.R. Bratt, Seismic detection capability at NORESS and implications for the detection threshold of a hypothetical network in the Soviet Union, *J. Geophys. Res.*, 94, 10,397-10,414, 1989.

Taylor, S.R. and H.E Hartse, Regional phase seismic detection thresholds at WMQ, *Los Alamos National Laboratory, Los Alamos, NM*, LAUR-96-395, 7pp, 1996.

Taylor, S.R., Analysis of high-frequency P_g/L_g ratios from NTS explosions and western U.S. earthquakes, *Los Alamos National Laboratory, Los Alamos, NM*, LAUR-95-3142, submitted to *Bull. Seism. Soc. Am.*, 1995.

Man–Made Seismic Events?, NW China

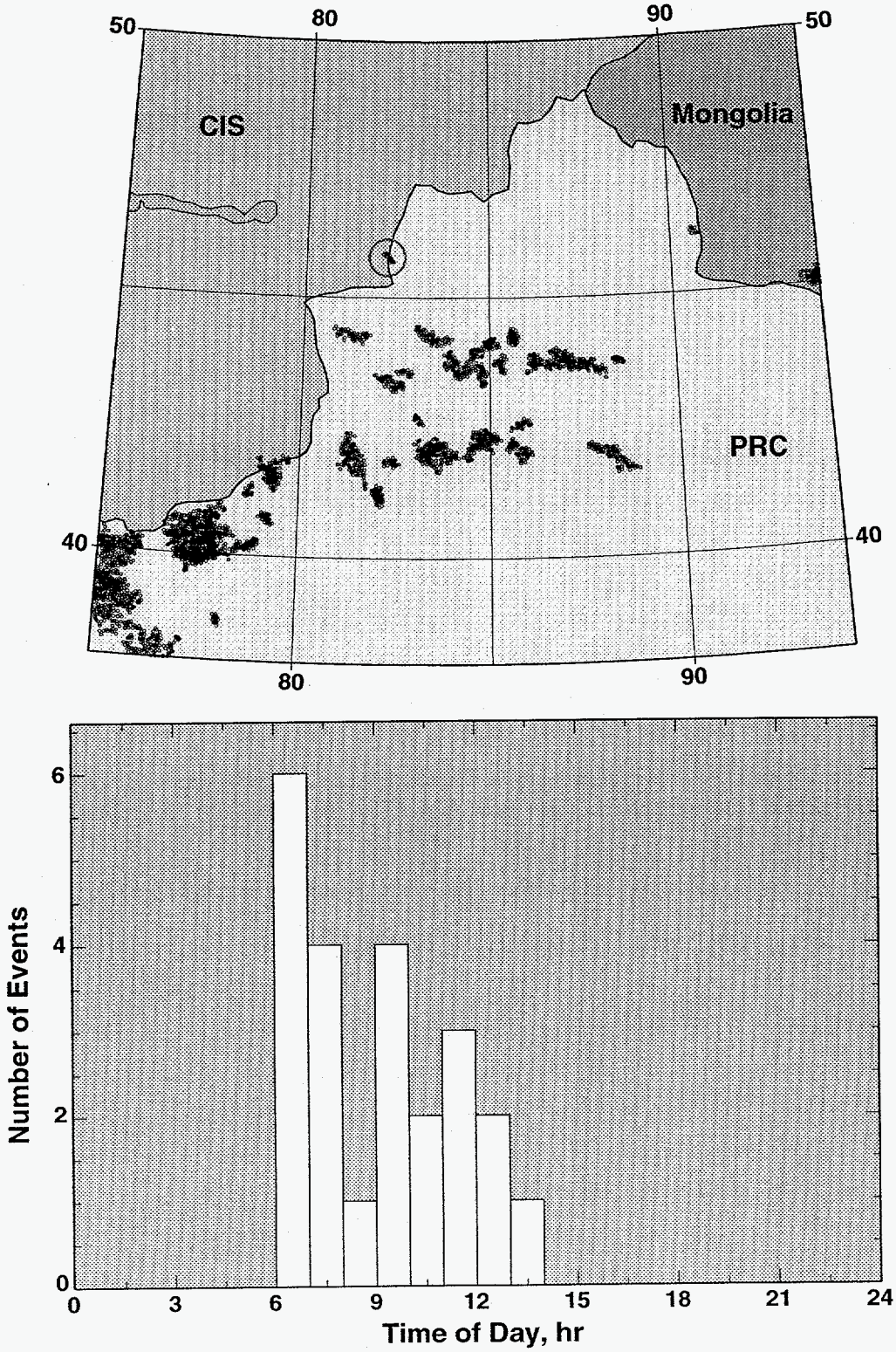

Figure 1. Map shows spatial clusters of seismicity for events from Chinese seismicity catalogs. The circled cluster on the Chinese border has a distinctive temporal clustering that suggested the events are mine blasts. We are trying to confirm this with overhead imagery and obtain a precise location.

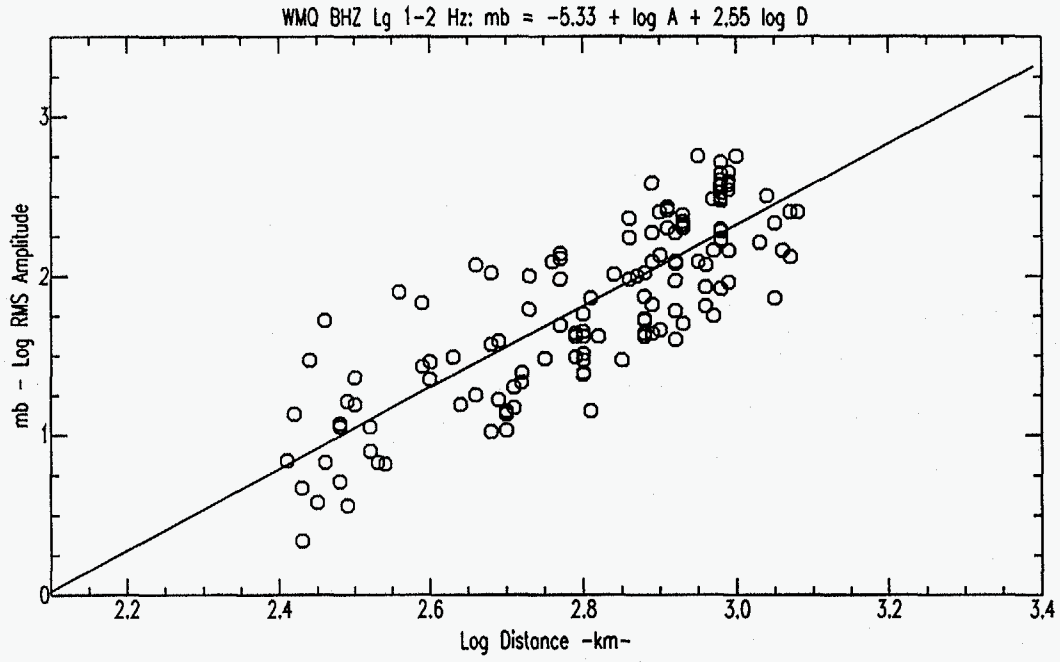

(a)

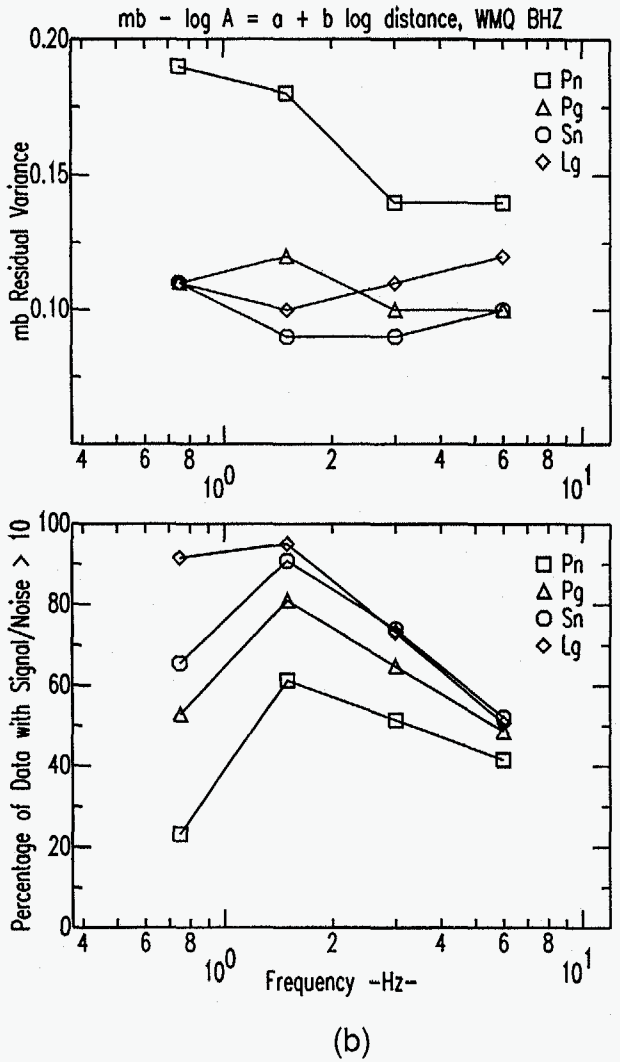

(b)

Figure 2. Results of a linear regression to calibrate a magnitude scale are shown in part a using Lg phase. In part b the results for the phases Pn, Pg, Sn, and Lg are shown for 4 passbands. Both the variance of the residual mb after claibration and the percentage of events that pass a signal to noise ratio test are shown.

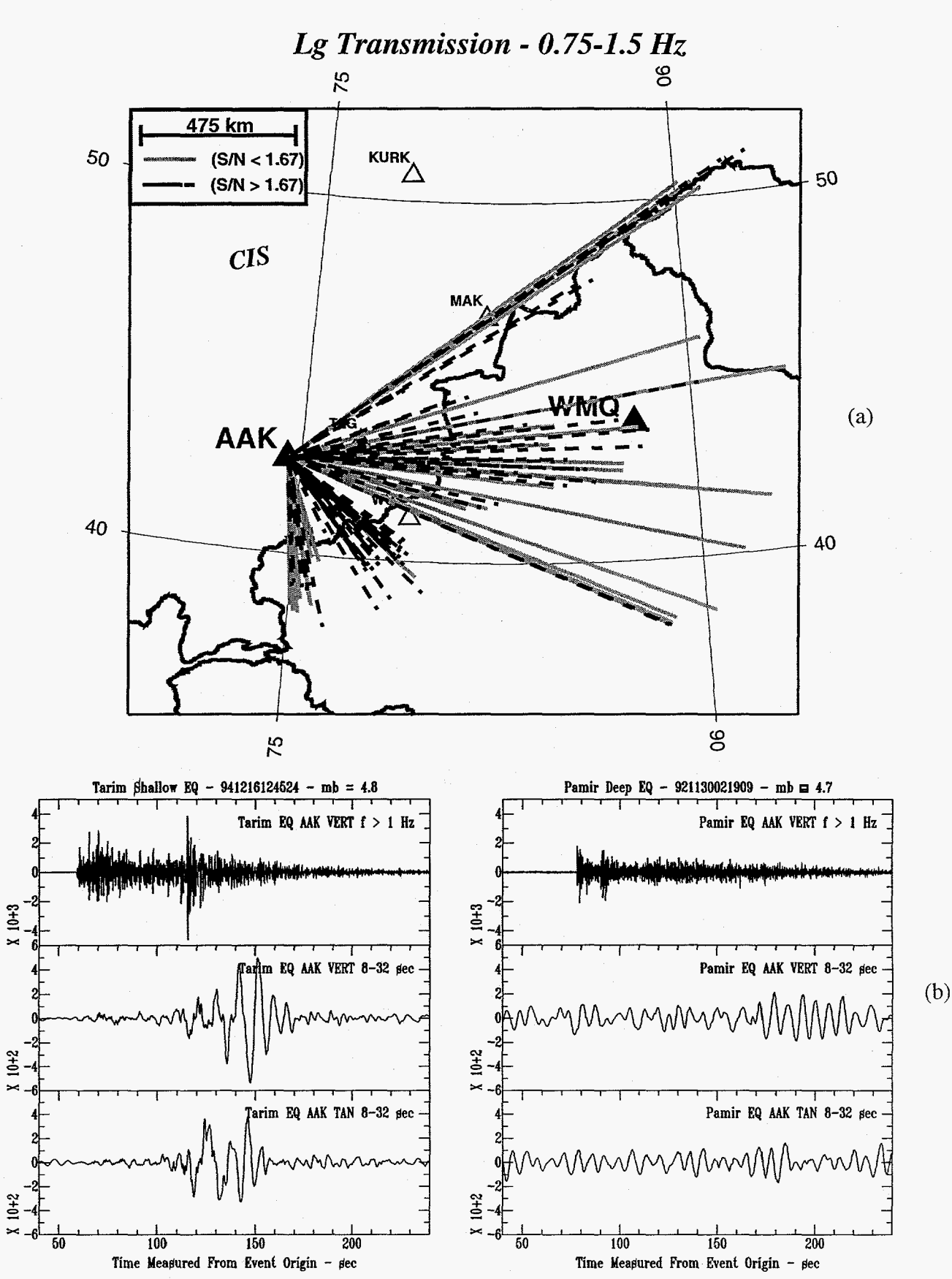

Figure 3. In part a, the map shows paths with strong and weak Lg propagation observed at station AAK. Paths to the south of AAK show both strong and weak Lg in a small region, suggesting that the change is too abrupt to be a path effect. In part b the short period vertical and long period vertical and tangential waveforms show no surface wave excitation with poor Lg, suggesting a deep source.

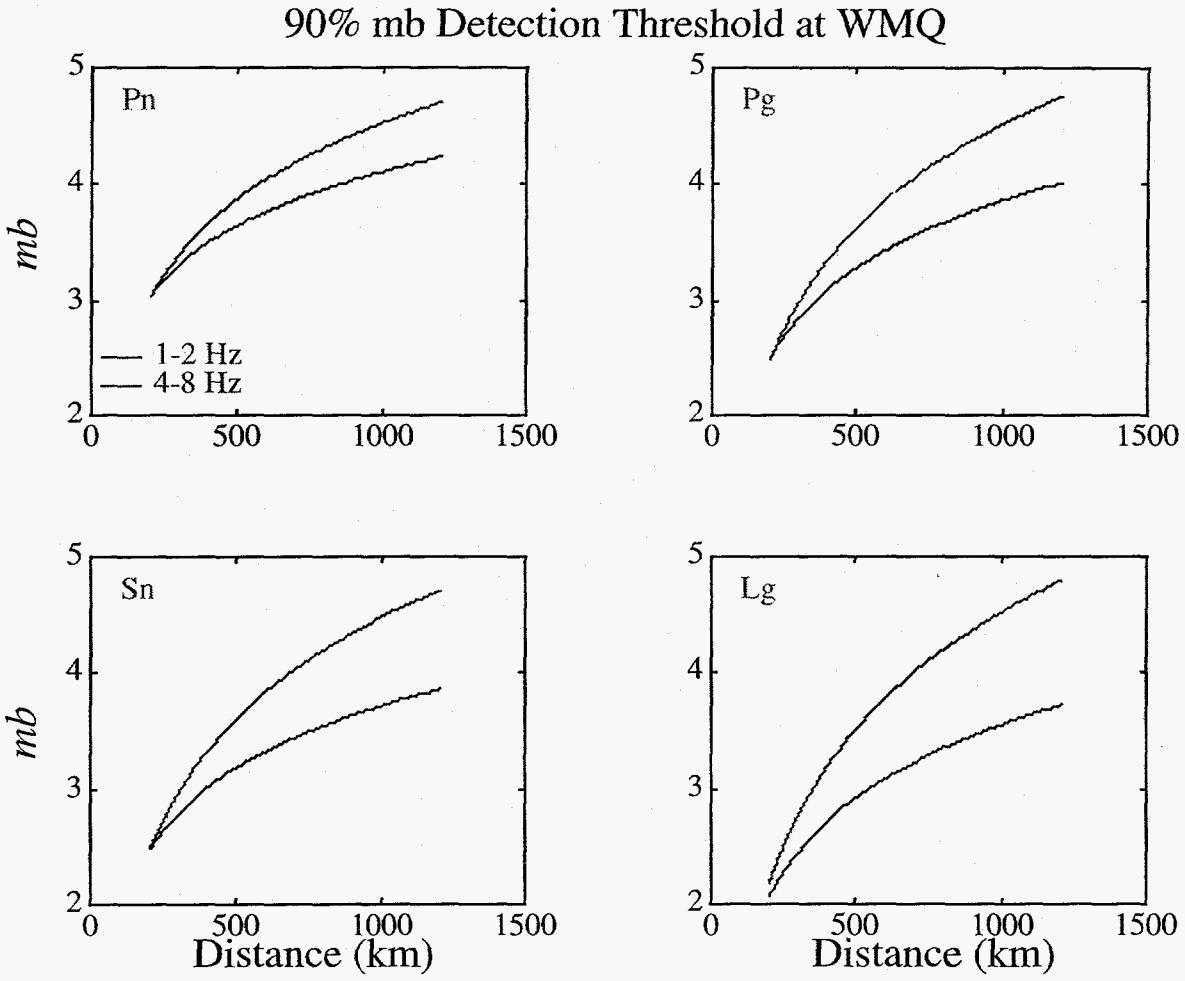

Figure 4. 90% detection thresholds for earthquakes recorded at WMQ for the phases Pn, Pg, Sn, and Lg in the 1-2 and 4-8 Hz bands.